Hindawi
Advances in Polymer Technology
Volume 2022, Article ID 5950215, 17 pages
https://doi.org/10.1155/2022/5950215

Research Article

Effect of Nanoclay Filler on Fatigue Life of Natural Rubber/Styrene-Butadiene Blend

Ali Bakhshizade, Ahmad Ghasemi-Ghalebahman, and Mohammad Ali Hajimousa

Faculty of Mechanical Engineering, Semnan University, P.O.B. 35131-19111, Semnan, Iran

Correspondence should be addressed to Ahmad Ghasemi-Ghalebahman; ghasemi@semnan.ac.ir

Received 5 March 2022; Revised 18 April 2022; Accepted 9 May 2022; Published 28 May 2022

Academic Editor: Anil K. Bhowmick

In this paper, the fatigue life of natural rubber (NR)/styrene-butadiene rubber (SBR) compound is evaluated experimentally. The parameters investigated are the NR, SBR, and nanoclay loading in the composition, strain amplitude, and the frequency of the fatigue test. Fracture surfaces of NR/SBR/nanoclay compound are investigated using scanning electron microscopy (SEM). The results show that by increasing NR and the nanoclay loading in the rubber composition, the fatigue life of the rubber increases. For the nanoclay, a threshold value exists beyond which the fatigue life of the rubber compound decreases. It is also observed that by increasing the test frequency, the fatigue life of the rubber compound decreased. Tensile, hardness, and dynamic mechanical thermal analysis (DMTA) tests were also performed to evaluate the mechanical and thermal properties of the compound. SEM results show that by increasing the strain amplitude, the test specimens fail softly, and the addition of nanoparticles roughens the fracture surface and increases the fatigue life.

1. Introduction

Mechanical properties of rubber materials play an important role in predicting the fatigue life of rotating parts in industrial machinery such as the automotive industry. It is worth noting that some parts of heavy vehicles are not easily replaced in the periodic maintenance service, and not knowing their service life can in some cases increase the maintenance costs of this equipment. On the other hand, the characteristics of long fatigue life, as well as high energy absorption and damping properties in rubber parts, increase the safety and reliability of industrial machines. Various factors affect the mechanical properties and fatigue life of rubber materials, including the type and amount of filler, the main polymer, chemical composition, operating conditions, and environment [1, 2]. Natural rubber (NR) has excellent tensile and tear strengths and good abrasion resistance for the production of tires, conveyor belts, fluid transfer systems, body sealing, car suspension, seals, adhesives, coatings, and body parts. In addition, NR has high fatigue strength in comparison to other rubbers [3]. This behavior makes NR a unique elastomer for the manufacturing of tires [4, 5]. NR is a polymer, a long, chain-like molecule that contains repeating subunits. The chemical name for NR is polyisoprene [6]. The monomer from which it is built is isoprene. Polyisoprenes can feature four different isomers in their polymer chain. These are cis-1,4; trans-1,4; 1,2; and 3,4. Isomers contain the same number of atoms of each element but have a different arrangement of those atoms. The numbers in the isomer name refer to the particular carbon atom in each unit, which is attached to adjacent units. NR consists almost entirely of the cis-1,4 structure and hence is, chemically, cis-1,4 polyisoprene. When the chain units in a polymer consist of the same isomer, it is said to be stereoregular. It is this stereoregularity, the almost 100% cis-1,4 polyisoprene structure of NR that gives many desirable mechanical properties to goods produced containing NR [6]. Many efforts have been made to improve the fatigue properties of NR products [7, 8]. The type, content, and dispersion of nanofillers have a significant effect on the microstructural, static, dynamic, and fatigue properties of rubber composites [9, 10]. In general, rubber fatigue involves a period time during which cracks, due to oscillating loading, initiate in areas that are not visible at first, and then grow and leading to the failure of the component over time. There are two distinct methods in the analysis of

rubber fatigue: crack initiation and crack propagation method [11]. Zhan et al. [12] investigated the crack growth resistance of NR reinforced with carbon nanotubes (CNTs) and concluded that the crack growth resistance of CNTs/NR composites is significantly higher than that of pure NR, and it has higher energy dissipation. The CNTs at the crack tip lead to a crack branching at low fatigue strain, which improves the crack growth resistance of CNTs/NR composites.

Due to the unfavorable mechanical properties of the rubber, the use of reinforcements inside the tires to increase their strength is essential. One of the most common additives is carbon black (CB). Various methods for the improvement of the dispersion of CB and increasing its efficiency have been proposed. One of these methods is the use of silicon, which has some advantages over CB. However, silicon has lower reactivity relative to CB, and this increases the curing time of the tire. Carbon black, nanoclay, and silica are commonly used to modify the structure and increase the dynamic properties of rubber materials. In recent decades, nanoclay has been used as a reinforcing filler for rubber to prepare rubber/nanoclay compounds. These are used in latex rubber [13, 14], solution blending [15–17], and melting compound [18–20].

Styrene-butadiene rubber (SBR) is known as a nonstrain-induced crystallization. This feature makes a significant difference in the mechanical properties of NR. SBR has lower tensile strength and tear strength, and reinforcement of all SBR compounds is required for use in engineering applications. Fillers such as carbon black are used to improve the mechanical properties [21]. Wu et al. [21] showed that the flexural fatigue life of CB-filled SBR is greatly enhanced by the addition of nanoclay. They showed that the addition of nanoclay did not reduce the crosslinking of the rubber compound, but increased the tearing energy. Observation of SEM images of fracture morphology in this study showed that nanoclay particles are superior to CB because they can blunt the crack tip. Nanoclay is a material with excellent reinforcement performance due to its high aspect ratio and good properties. SBR was prepared with a mixture of CB and nanoclay. With this composition, hysteresis and rupture energy were improved. The fatigue life of SBR nanocomposite was improved by increasing the amount of nanoclay. Dong et al. [22] showed that NR filled with CB shows the best resistance to quasistatic fracture and dynamic crack growth resistance among carbon-based nanofillers in NR. It also has the highest amount of developed strain, which eliminates most of the local input energy and then improves fatigue resistance. Liu et al. [23] claimed that NR containing CB and nanoclay had excellent mechanical properties and better fatigue resistance. Burgaz et al. [24] investigated fatigue behavior and dynamic mechanical properties of NR/SBR and NR/SBR/CB rubbers. They showed that the addition of butadiene rubber (BR) improved the fatigue resistance of NR/SBR 4-5 times. The results of SEM in this study showed that the fracture surfaces of the NR/CB have brittle and relatively sharp fracture surfaces compared to NR/BR/CB composite. Because BR has more elasticity than NR/BR composition, it has a soft fracture process, and crack growth is much more difficult than pure NR. In terms of viscosity, the combination of NR reinforced with CB or a combination of NR/SBR has different degrees of viscosity. NR composites can be used as antivibration rubber bush in automotive applications where fatigue resistance is expected to be high. Rooj et al. [25] created a network of CB and nanoclay particles in NR. The crack growth rate decreased in the presence of nanoparticles. Gopi et al. [26] investigated the use of SBR/CB/nanoclay nanocomposite in the tire tread. SBR/nanoclay nanocomposite was prepared by a melt intercalation system. The results of the dynamic analysis showed that the new composition has higher rolling resistance and moisture absorption. In a study by Chang Su et al. [27], acrylonitrile-butadiene rubber (NBR) was used in combination with zinc oxide and stearic acid; sulfur with a purity of 99.9% is used as a bonding agent; TT and CZ accelerators were also used, and CB-nanoclay mixture and nanoclay were used. The mechanical properties of different nanocomposites based on the type of nanoclay and the abundance of additives showed that the hardness and elongation at the fracture point depend on the amount of clay. Also, the thermal and dynamic properties of the fabricated composition were superior to the properties of NR. Li et al. [28] investigated the effect of a crystalline copolymer that can be bonded to a polymer network and the dispersion of filler CB/NR/SBR nanocomposites. Their results showed that nanocomposites incorporated with crystalline copolymer by increasing the heat and rolling reduce the resistance to abrasion and fatigue. Cheng et al. [29] significantly improved thermal conductivity by fabricating covalently bonded silicon carbide nanowires arranged vertically in NR.

In the study of Izadi et al. [30], the NBR/nanoclay composite was prepared by melt intercalation in an internal mixer. Various mechanical and thermal tests were performed to evaluate the performance of the elastomeric stator lining of downhole mud motors. The results of the tensile test showed that the stiffness and toughness of the prepared composites increase simultaneously. While the results of the tensile fatigue test showed an increase in fatigue life of NBR/nanoclay composite samples compared to pure NBR samples. Based on their results, it was confirmed that the integration of nanoclay in the NBR matrix increases the mechanical and thermal strength compared to the virgin elastomer. Dutta et al. [31] investigated the nanoclay distribution between two phases of a new class of dynamically vulcanized TPV based on POE/EVA (polyethylene octane elastomer/ethylene vinyl acetate) elastomers. Elastomer was combined with different amounts of organic clay (0.5, 1, and 3 wt %). Dicomyl peroxide (DCP) was used as a vulcanizing agent in the melt mixing process. The effects of organic clay on mechanical properties, swelling kinetics, crystallization, vulcanization properties, dynamic mechanical behavior, electrical properties, and morphology were investigated. XRD analysis showed a decrease in crystallinity by adding EVA to the POE matrix. The morphological observations of the fracture surface showed that the smaller EVA domain was distributed quite uniformly in the POE phase, and the clay phase was mainly distributed in the EVA phase. Swelling properties, electrical properties, and storage modulus were also improved with clay for a composition containing higher EVA content. The study of the Rajeshkumar et al. [32] is an overview of the different types and properties of natural fibers, polymers, nanolayers, and natural nanoclay-added natural fiber composites according to their mechanical properties. The nanoclay-added composites offer improved properties due to the enrichment of the

Table 1: Types of samples used in fatigue testing.

Row	Chemical composition	Nanoclay (phr)	SBR (phr)	NR (phr)
1	S70N30	—	70	30
2	S50N50	—	50	50
3	S40N60	—	40	60
4	S50N50C5	5	50	50
5	S40N60C3	3	40	60
6	S40N60C5	5	40	60
7	S40N60C7	7	40	60

Table 2: Chemical composition of rubber samples.

Row	Chemical material	Amount (phr)
1	NR	60
2	SBR	40
3	4010 NA[1]	1
4	Stearic acid (Sta)	1.5
5	Zinc oxide (ZnO)	5
6	TMQ	0.8
7	Sulfur (S)	1
8	Accelerator [2] (MBTS)	2
9	Accelerator [3] (CZ)	2
10	Nanoclay	3, 5, 7

The test samples are prepared according to the ASTM D412 standard. Fatigue tests are performed according to ISO 6943 standard at 3 Hz frequency. [1]N-Isopropyl-N′-pheny1-4-Phenylenediamine. [2]N-Cyclohexyl-2-benzothiazole sulfonamide (CBS). [3]2-2′-Dithiobis (benzothiazole).

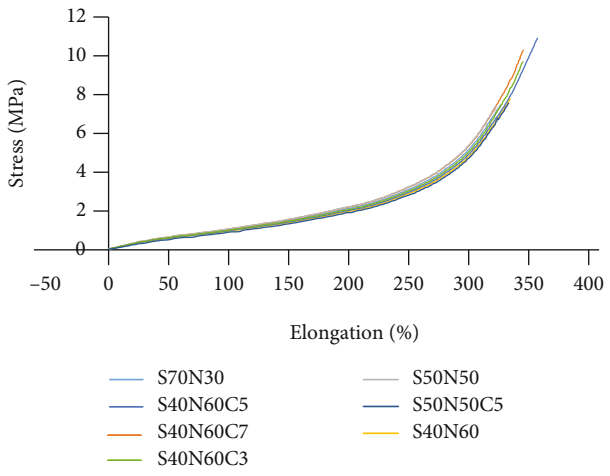

Figure 1: Stress changes in terms of elongation of the samples.

interfacial bonding between the matrix and the reinforcing materials. In addition, nanoclay can increase the flexibility and strength of natural fibers in a single phase. Zdiri et al. [33] studied the effect of Tunisian clay filler on the rheological and thermal behaviors of based recycled polypropylene (RPP) composites. RPP was mixed with 1, 3, 5, and 7 wt% of clay particles using a two-screw extruder. Fourier transform infrared spectroscopy (FTIR) analysis showed that clay particles altered the shape of the observation band of RPP, denoting the attendance of a chemical interaction between the clay and RPP matrix. Increased storage modulus and loss modulus indicated the reinforcing effect of clay filler on the RPP matrix. With increasing clay loading, the melting temperature decreased, and the crystallization temperature increased. A study was conducted by Prusty et al. [34] to investigate the design of polyethylhexyl acrylate/polyvinyl alcohol (Sg-PEHA/PVA/nanoclay) thin films. The presence of exfoliated nanoclay throughout the films was demonstrated by field emission scanning electron microscopy images. It was observed that the tensile strength, thermal conductivity, thermal properties, and refractive index of thin films increased with increasing Cloisite30B content due to the formation of the exfoliated and partially fragmented structure of Sg-PEHA/PVA/nanoclay. Due to the sandwich structure of the clay platelets, the oxygen obstacle properties of the thin films were reduced fivefold.

Despite many studies on improving the fatigue life of NR using various additives, the study of fatigue life of NR/SBR compounds is still of interest among researchers in this field. In this study, the effect of nanoclay additive, strain value, and natural frequency on the fatigue life of NR/SBR was investigated.

2. Experimental Studies

2.1. Materials. The materials used in this research are SMR20 natural rubber made in Malaysia, which is widely used in various industries [8], styrene-butadiene 1502 grade with 23.5 wt% styrene and 76.5 wt% butadiene made by Imam Port Petrochemical Iran with a glass transition temperature of -58°C [36]. Compounding components which include N-cyclohexyl-2-benzothiazole sulfenamide (CBS), 2-2′-dithiobis benzothiazole (CZ), sulfur (S), zinc oxide (ZnO), and stearic acid were commercial grade products and used as received. Nanoclay additive used in this research is k10 montmorillonite type from Sigma-Aldrich Germany with a density of 0.5-0.7 g/cm^3, and cation exchange capacity is 48 meq/100gr.

2.2. Compound and Preparation of Samples. The two-roller mill is used at the beginning of the manufacturing process to reduce the viscosity of the base rubber and then to mix the curing agents and accelerators with the base rubber. In this research, the laboratory roller Brabender PM300 model made in Germany has been used. The rollers of this machine have diameters of 4 inches and 8 inches and the distance between them can be adjusted in the range of 0.005 to 0.195 inches. The compounds are prepared at 30°C. The friction ratio of the mixing process was 1 : 3.

To prepare the mixture, first, the NR and SBR base materials were combined with the weight ratio specified in Table 1 on a double mill with stearic acid, ZnO, 4010NA, and TMQ for approximately 15 minutes according to the values in Table 2. The zinc oxide and stearic acid are considered activators; they activate intermediate reactions. After that, the curing agents including sulfur and CZ and MBTS accelerators were added to the previous compound according to the data in Table 2, and the compound was mixed for approximately 15 minutes. Mixing was continued until the torque mixing

Table 3: Mechanical properties of different rubber samples.

Row	Chemical material	Hardness (shore A)	Mean values of the tensile strength (MPa)	Standard deviation values	Mean values of tear strength (N/mm)	Standard deviation values
1	S70N30	44	6.78	0.86	11.23	0.96
2	S50N50	47	7.21	2.03	14.54	0.67
3	S40N60	49	7.82	0.58	19.07	1.14
4	S50N50C5	49	7.66	0.73	15.78	0.31
5	S40N60C3	51	9.73	0.62	16.87	0.17
6	S40N60C5	53	10.81	0.40	21.72	1.59
7	S40N60C7	52	10.24	1.25	20.16	2.11

reached the steady-state level. After mixing and achieving the composition of raw materials, the curing time was obtained using a rheometer. Finally, using the torque-time diagram obtained from the rheometer, the optimal curing time of the mixture can be obtained. Monsanto 100S oscillating disc rheometer made in England is used. The curing characteristic of the prepared compound at 160° C is determined according to the ASTM D5289 standard. The samples were placed in a mold under a hydraulic press model 400S Polystat made in Germany under a pressure of 60 bar and a temperature of 160°C, and rubber plates with dimensions of 20 × 20 cm and a thickness of 1.5 mm are obtained.

To make rubber plates containing nanoclays, it was necessary to disperse the nanoparticles in the base rubber and then continue the manufacturing process. The only difference in the construction of rubber plates containing nanoparticles is the diffusion of nanoparticles into the base rubber. It should be noted that before the nanoparticle dispersion process inside the base rubber, the nanoclay is placed in an oven at 60°C for 24 hours to remove any possible moisture absorbed by nanoclay. Also, for dispersing nanoparticles, an internal mixing device consisting of two spiral blades was used. The nanoparticles and base rubbers were passed, for a certain duration and rotational speed through this mixing device. The shear force is applied to the mixture which causes the nanoparticles clusters to open and disperse. The internal mixer temperature is set to 150°C, and its rotational speed is 80 rpm, and the mixing time is 18 minutes. After the nanoparticle dispersion process is completed by the internal mixer, the rubber and nanoclay mixture is rested for at least 30 minutes to reduce the residual stress while reducing the temperature of the compound. After that, the curing agents and other additives were mixed with rubber-containing nanoclays using rollers, and according to the information obtained from the rheometer, the rubber was placed inside the press machine, and rubber plates with dimensions of 20 × 20 cm and thickness of 1.5 mm were obtained.

Therefore, the different types of rubber samples studied in this research are in Table 1.

The chemical composition of different materials used in the rubber composition and its additives are summarized in Table 2. It is worth noting that the amount of nanoclay additive in rubber compounds varies, while the ratio of other components is kept constant.

The tensile mechanical properties are obtained by using the HIWA 200 tensile testing machine made in Iran with a crosshead speed of 500 mm/min. The tensile tests are repeated 3 times for each composition listed in Table 1.

Fatigue tests are performed at 50%, 60%, and 70% [38] strain amplitude and for 3 samples at each strain amplitude, and from 7 types of chemical compositions listed in Table 1. It is worth mentioning that the model of the device used for fatigue testing is HIWA 600 made in Iran. It can test six samples, simultaneously.

Then, scanning electron microscopy (SEM) images are also taken from fracture surfaces to study the failure surfaces and morphology of the material. The SEM used in this research was the MIRA III model made by the TESCAN company in the Czech Republic.

The dynamic mechanical thermal spectra of the compounds were obtained by using a DMA-Triton, model Tritec 2000 made in England. These tests were analyzed in the tension mode at a constant frequency of 1 Hz, a displacement of 0.05 mm, over a temperature range from -90°C to 70°C, at a heating rate of 5°C/min. Storage modulus and dynamic loss factor were measured as a function of temperature for all the samples. The temperature corresponding to the peak in the tanδ versus temperature plot was taken as the glass transition temperature (Tg).

3. Results and Discussion

The stress changes in terms of elongation of the samples are also under Figure 1. As can be seen, by reducing the amount of NR in the rubber composition, the amount of toughness of the material decreases, and its strength increases. Another important point is that adding nanoclays to the rubber compound will reduce the amount of elongation and consequently the toughness of the rubber compound.

Table 3 also shows the mechanical properties of the rubber compositions made. As the amount of NR in the composition increases, so does the amount of hardness, tear strength, and tensile strength. These results can show an enhanced fracture resistance with increasing content of NR and nanoclay.

The fatigue life of specimens with compounds S70N30, S50N50, and S40N60 at different strain values are shown in Figure 2. As can be seen, by increasing the amount of NR in the composition from 30 to 60 phr, the fatigue life of rubber compounds is more than doubled. This shows that the presence of NR increases the fatigue life of rubber compounds.

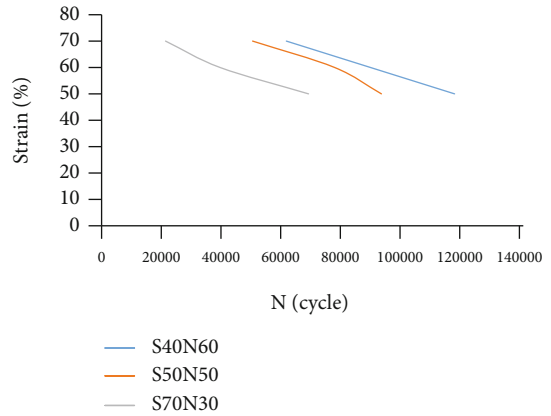

Figure 2: Strain-life of the different compounds at 50%, 60%, and 70% strain amplitude.

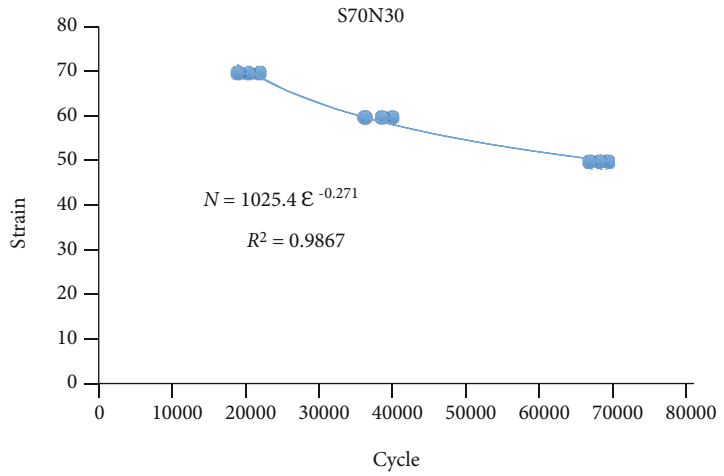

Figure 3: Fitted curve error in the strain-life diagram of S70N30 compound.

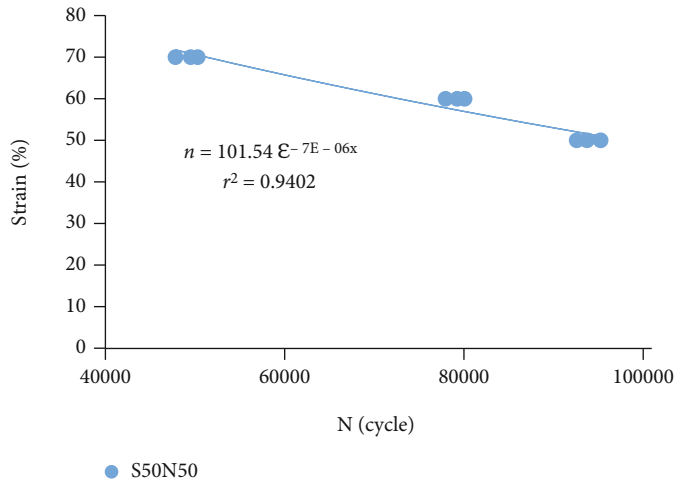

Figure 4: Fitted curve error in the strain-life diagram of S50N50 compound.

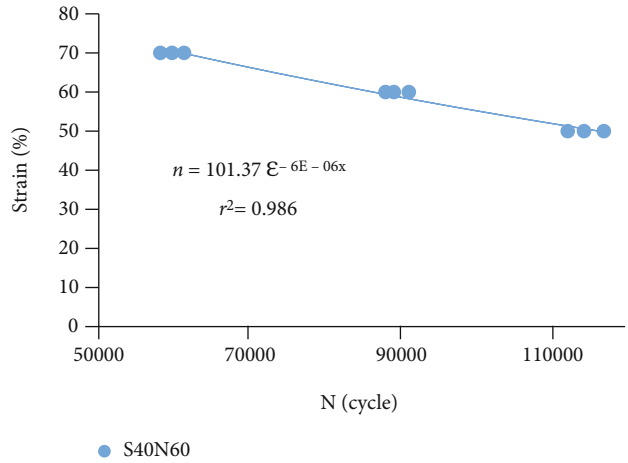

Figure 5: Fitted curve error in the strain-life diagram of S40N60 compound.

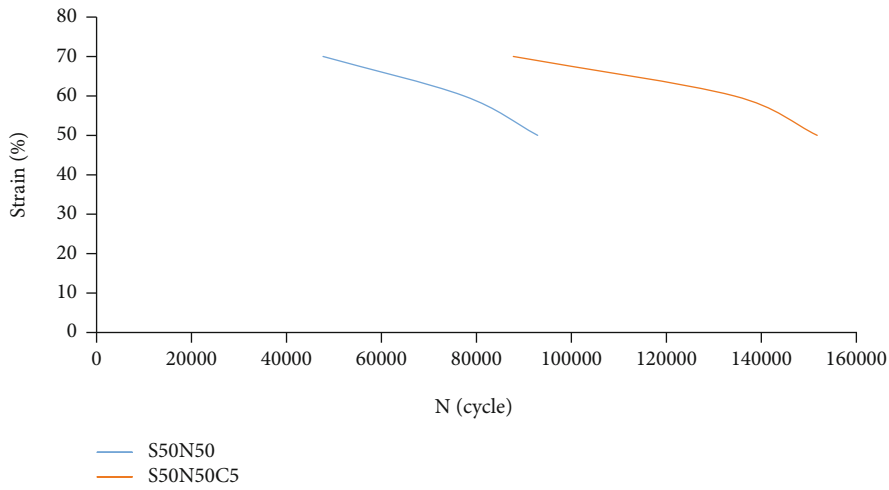

Figure 6: Strain-life diagram of the S50N50 and S50N50 C5 compounds with nanoclay.

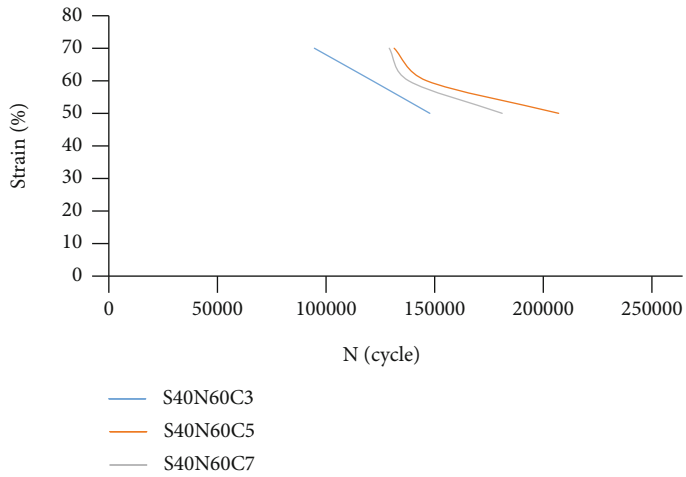

Figure 7: Stain-life of the different compounds with different loading of nanoclay.

Table 4: Rubber fatigue life with different properties at 50%, 60%, and 70% strain values.

Strain (%)	Specimen number	*N* (cycle)						
		S70N30	S50N50	S40N60	S50N50C5	S40N60C3	S40N60C5	S40N60C7
50	1	68693	92890	117180	151762	145632	204096	178463
	2	67521	91762	114531	150078	142793	207661	176520
	3	66207	94385	112375	147326	140066	206889	179827
60	1	39320	77351	89243	134261	119612	144205	136029
	2	37983	78629	88127	133556	118720	145430	132157
	3	35632	79443	91246	131040	117241	141097	134763
70	1	21232	50131	61339	84239	93261	129461	127231
	2	19734	49362	59748	86521	94567	128554	122869
	3	18283	47695	58183	87766	91342	126293	124076

Table 5: Standard deviation values according to the fatigue life test of samples.

Strain (%)	Standard deviation values						
	S70N30	S50N50	S40N60	S50N50C5	S40N60C3	S40N60C5	S40N60C7
50	1243.676	2627.718	2123.513	4339.569	2725.35	1266.111	1693.501
60	1867.088	1444.622	633.862	1259.162	1806.592	1397.122	1904.621
70	1474.562	2191.735	1482.366	795.8247	1741.522	1967.907	2756.195

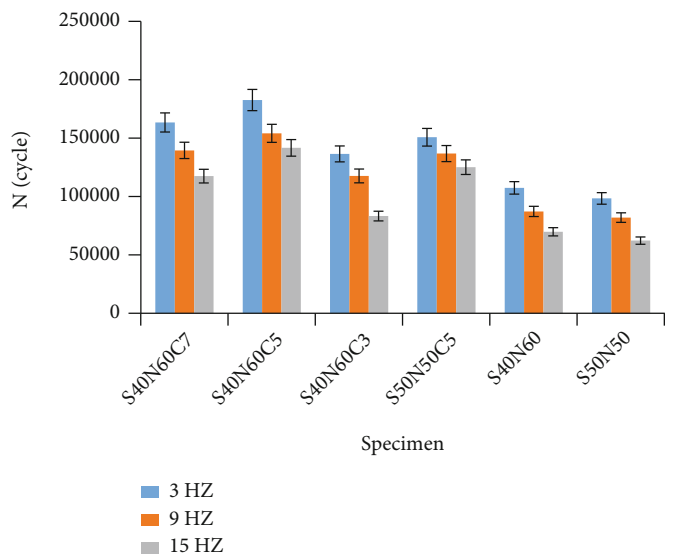

Figure 8: Fatigue life changes of different samples at 50% strain and at frequencies of 3 Hz, 9 Hz, and 15 Hz.

The crystallinity of NR is a characteristic provided by the microstructure. If the units of a polymer chain are in a regular enough spatial arrangement, then interactions between these units from polar attraction, hydrogen bonding, or functional groups, will form crystalline structures which stiffen the polymer. NR, because of its stereoregularity, will form crystallites upon storage and upon stretching. Although crystallization upon storage can cause some processing difficulties, the reversible crystallization upon stretching, so-called strain-induced crystallization, caused by intermolecular forces in the polymer, provides many of the unique properties of NR. In the final product, strain-induced crystallization results in excellent cut resistance, tear resistance, tensile strength, and crack growth resistance [39, 43].

Also, as the amount of strain decreases, the fatigue life of the specimens increases exponentially. In addition, the fitted curve error is acceptable in all samples. The values of R^2 in Figures 3–5, showing the error of the curve fitting of the

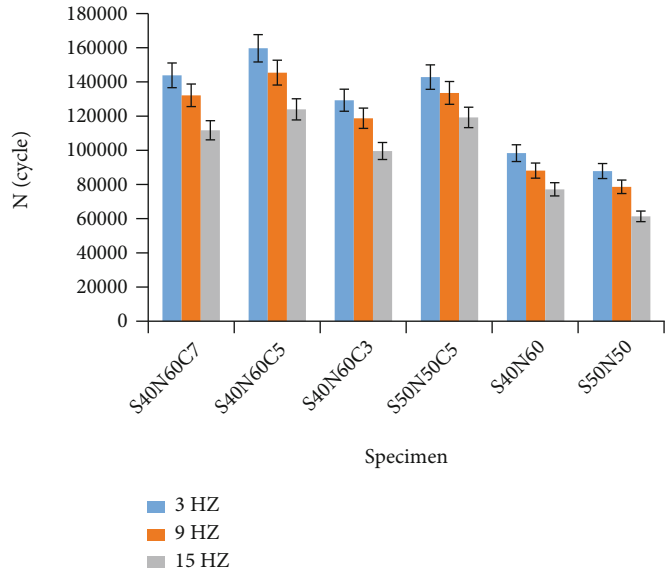

Figure 9: Fatigue life changes of different samples at 60% strain and at frequencies of 3 Hz, 9 Hz, and 15 Hz.

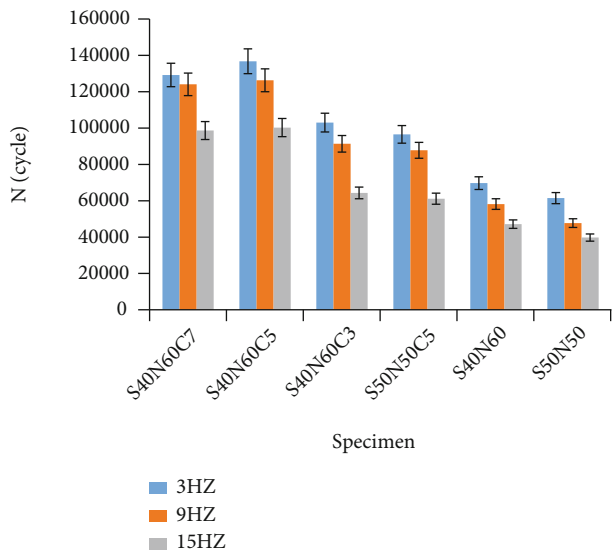

Figure 10: Fatigue life changes of different samples at 70% strain and frequencies of 3 Hz, 9 Hz, and 15 Hz.

strain-life curves, are negligible. Some authors have used the strain parameter as a damage factor in the analysis of fatigue life [39, 40, 41].

Nanoclay at 3, 5, and 7 phr loading was also added to different rubber compounds, and their fatigue life at different strain values was investigated. The fatigue life of S50N50 and S50N50C5 rubber compounds at 50%, 60%, and 70% strain amplitude are shown in Figure 6. As can be seen, by adding 5 phr of nanoclay to the S50N50 rubber compound, the fatigue life of the rubber is increased by a minimum value of 50% and a maximum value of 80%. Due to the structural composition of the nanoclay, it is possible to improve the thermodynamic reactions between the rubber polymer chains and the nanoclay silicate layers, which ultimately leads to better nanoclay diffusion within the polymer network. It can be stated that the use of nanoclay in rubber composition has not only improved the mechanical properties and fatigue life of rubber but also its thermal properties [44].

Then, by adding nanoclay of 3, 5, and 7 phr loading to different rubber compositions, their fatigue life at different strains is investigated. The fatigue life of S40N60C3, S40N60C5, and S40N60C7 rubber compounds carried out at 50%, 60%, and 70% strains are shown in Figure 7. Comparing these results with those shown in Figure 2, it is concluded that the addition of 3 phr of nanoclay to the S40N60 rubber compound increased the fatigue life by at least 24% and at maximum by 57%. The addition of 5 phr of nanoclay loading to the S40N60 rubber compound resulted in an increase of a minimum of 54 to a maximum of 117 in the fatigue life of the rubber. It is worth noting that by increasing the nanoclay loading to 7 phr, the fatigue life of the S40N60 rubber compound increased by a minimum of 47% and a maximum of 113%. Therefore, although the addition of nanoclay to the S40N60 rubber compound significantly increases the fatigue life of the rubber, increasing more than 5 phr of nanoclay in the composition will not change the fatigue life of the rubber. The weaker fatigue resistance of the composite filled with 7 phr nanomaterial was ascribed to its higher hysteresis, which resulted in heat generation under dynamic fatigue conditions [38]. Usually, in the cyclic fatigue test, hysteresis could decrease the energy available to be released by crack growth and then increase the fatigue resistance. However, a higher hysteresis might be adverse to fatigue properties. High temperatures due to heat accumulation can accelerate molecular chain rupture and repress strain-induced crystallization for crystalline rubber, such as NR, which can weaken the fatigue resistance of rubber materials [38]. It is noticeable that the fatigue life of the S40N60 rubber compound is much longer than that of the S50N50, indicating that increasing NR loading in the rubber compound increases the size of the crack tip

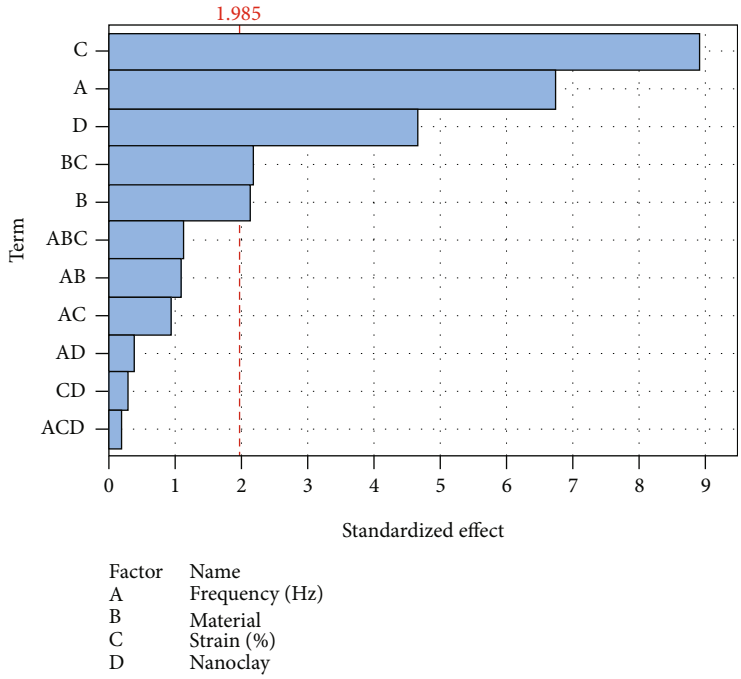

Figure 11: Sensitivity analysis of rubber fatigue life in terms of strain amplitude, amount of nanoclay in the composition, and test frequency parameters.

plastic zone and delays the crack growth. As a result, the life of the compound increases.

A summary of fatigue test results of different rubber compositions is presented in Table 4. It is observed that the addition of nanoclay to the combination of NR and SBR S40N60 significantly increases the fatigue life of the rubber. Adding 3, 5, and 7 phr of nanoclay to the mentioned rubber composition will increase the fatigue life of the rubber by 57%, 117%, and 113%, respectively. Therefore, the optimal amount of nanoclay additive to the S40N60 rubber compound is 5 phr, and adding more to the said rubber compound will not affect its fatigue life. On the other hand, it can be seen that adding 5 phr of nanoclay to S50N50 and S40N60 rubber compounds increases the fatigue life of the rubber compound by 80% and 117%, respectively. Therefore, it is concluded that the presence of 10 phr more NR in the rubber composition will increase the fatigue life of the rubber by 37% by adding 5 phr of nanoclay in the rubber composition. The standard deviation values are also presented in Table 5.

Another parameter affecting the fatigue life of various rubber compositions is the frequency of the fatigue test. In addition to the 3 Hz frequency, the fatigue tests were performed at higher frequencies of 9 Hz and 15 Hz. The results of the fatigue tests for various frequencies are shown in Figures 8–10 for 50%, 60%, and 70% strain. The results show that with increasing the frequency of the fatigue testing, the fatigue life of various rubber compounds is reduced. This is due to the production of more heat on the surface and inside the rubber specimens during the fatigue test at a higher frequency. Fatigue life is closely related to the crack growth characteristics of the material. Fatigue in some cases is caused by the propagation of cracks or unstable defects under cyclic loading. All rubber vulcanizations have a viscoelastic property that results in energy loss if exposed to a long cyclic deformation called dynamic residuals. Hysteresis leads to an increase in the temperature of the sample under cyclic stress fields. However, it has been shown that energy loss due to delayed crack growth increases tire vulcanization fatigue resistance [42].

Using the sensitivity analysis method, the effect of test frequency parameters, material composition, strain amplitude, and the amount of nanoclays added to the rubber composition on the fatigue life is investigated. For this purpose, the regression method and Pareto diagram are used. The Pareto diagram is used to highlight the most important parameter among a (usually large) set of parameters. In Pareto diagrams, out-of-reference effects (red line in Figure 11) have a significant effect on output changes. Sensitivity analysis of strain amplitude parameters, the amount of nanoclay additive in the rubber composition, and the test frequency according to Figure 11 show that among the various parameters, the strain amplitude and the amount of SBR/NR composition have the highest and lowest effect on fatigue life, respectively. It is worth noting that according to Figure 11, the combination of frequency, strain amplitude, and nanoclay effects will have the least effect on the fatigue life of rubbers.

The scatter of fatigue test data in terms of different rubber compositions in different strain amplitudes according to Figure 12 shows that the maximum and minimum scatter of fatigue life data are for 70% and 50% strain amplitudes, respectively. Also, an overview of the diagrams in the different strain amplitudes shows that the maximum and minimum scatter of fatigue life data are for S40N60C3 and S70N30 rubber samples, respectively.

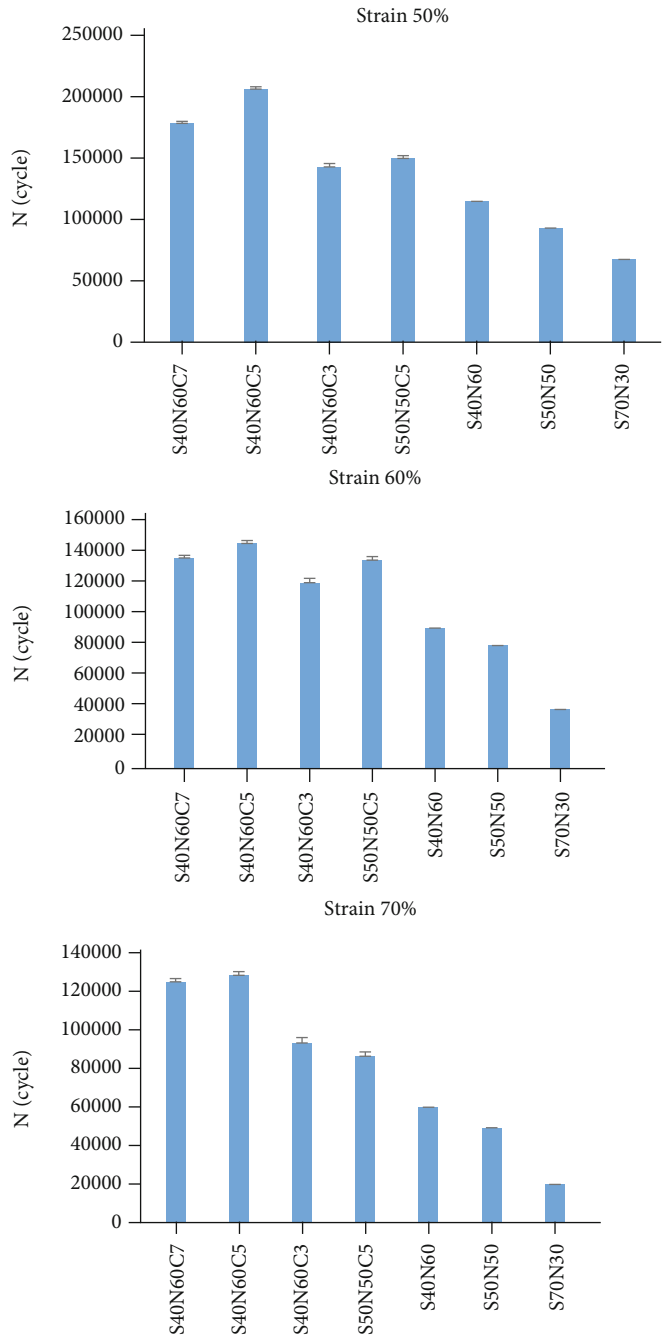

Figure 12: Investigation of fatigue test data scatter in terms of different rubber compositions in different strain amplitudes.

3.1. Microstructure Analysis. In this study, fatigue life experiments were performed at $R = 0$. At the macroscopic scale, the failure occurred perpendicularly to the stretching direction (damage mode 1), in the section of minimum width (the middle of the sample). Evaluation of the fracture surface on the microscopic scale after fatigue failure is important. In addition, fracture surface morphologies give some information about the failure process and mechanisms.

The results of SEM images with an accuracy of 50 μm are used to study the microstructure of different rubber compounds as well as their failure mechanism after performing fatigue tests. Figure 13 shows the failure surfaces of the S70N30 specimen at strain values of 50%, 60%, and 70%, respectively.

These photographs show that the fractured surface of these composites follows different mechanisms. The images (especially in the range of 50% and 60% strain amplitudes) revealed a relatively rough and uneven fractured surface, indicating that the samples failed in a ductile mode. It is observed that with increasing strain amplitude value, the fracture surface becomes smoother. The crack roughness is a characteristic of the crack growth rate [35]. The higher ratio of the macroscopic rough to smooth fracture surface

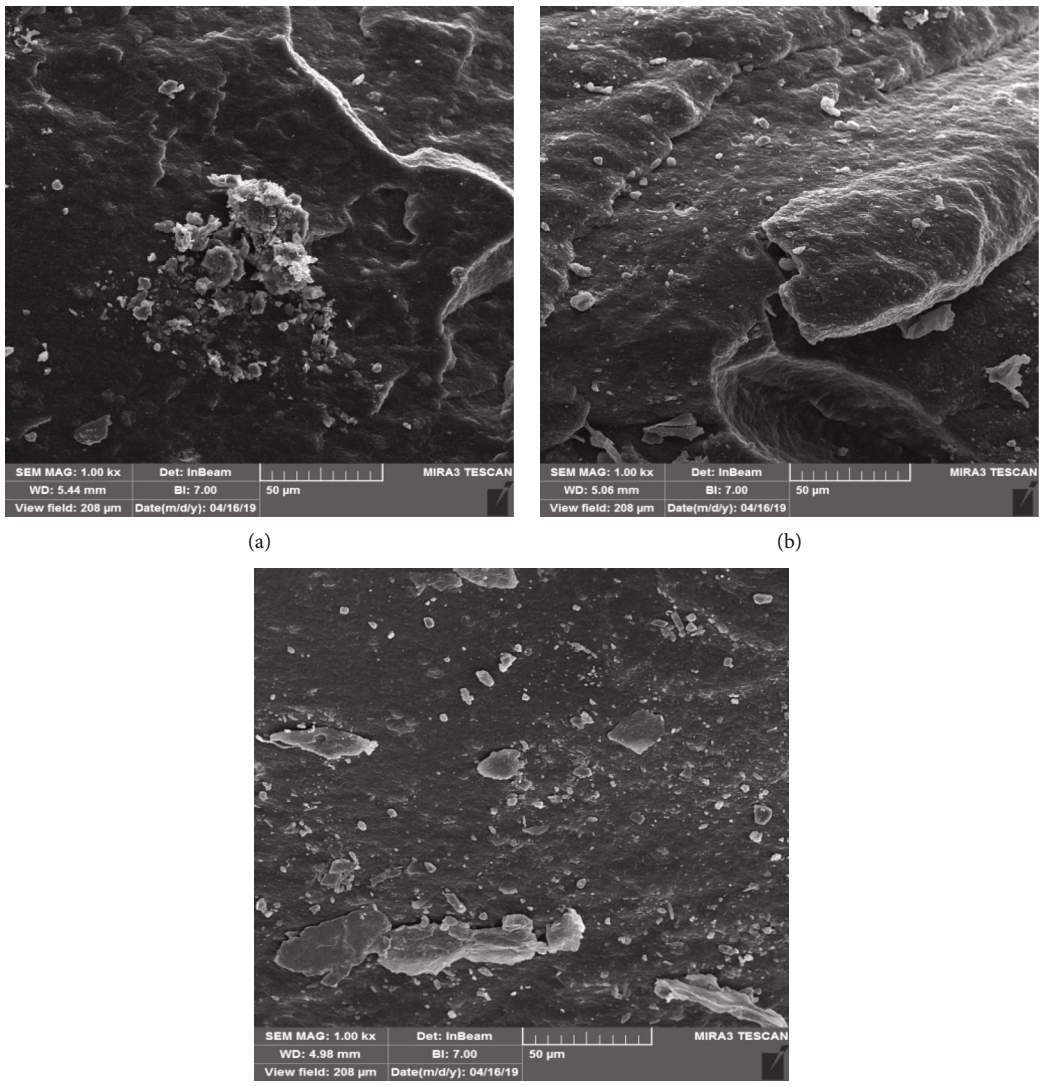

Figure 13: SEM image: (a) 50% strain amplitude for S70N30 sample, (b) 60% strain amplitude for S50N50C5 sample, and (c) 70% strain amplitude for S50N50C5 sample.

shows stronger resistance to crack growth. It is reported [38] that the microscopic smooth surfaces reflected less energy dissipation compared with microscopically rough crack surfaces. The smooth fracture surface indicates that the material failed in the brittle mode and also shows less elongation at the break value [46].

NR includes almost entirely of the cis-1,4 structure and so is, chemically, cis-1,4 polyisoprene. When the chain units in a polymer consist of the same isomer, it is said to be stereoregular. It is this stereoregularity, the nearly 100% cis-1,4 polyisoprene structure of NR, that admits many of the desirable properties to the mechanical goods NR is used to produce [6, 35]. The crystallinity of NR is a characteristic provided by this microstructure. If the units of a polymer chain are in a regular enough spatial arrangement, then interactions between these units from polar attraction, hydrogen bonding, or functional groups, will form crystalline structures which stiffen the polymer. NR, because of its stereoregularity, will form crystallites upon storage and upon stretching. Although crystallization upon storage can cause some processing difficulties, the reversible crystallization upon stretching, so-called strain-induced crystallization, caused by intermolecular forces in the polymer, provides many of the unique properties of NR. Specifically, these are its excellent green strength (uncured rubber strength) and building tack, both of which are of prime importance in tire building. In the final product, strain-induced crystallization results in excellent cut resistance, tear resistance, tensile strength, and cut and crack growth resistance [41].

There is more than just high cis content that furnishes the combination of rate and degree of crystallization performed by NR. In addition to the hydrocarbon portion, NR contains approximately 6% nonrubber constituents; ~2.2% proteins, ~3.4% lipids (fatty acids), glycolipids, and phospholipids, and ~0.4% carbohydrates [6]. It has been found that deproteinized NR still represents the crystallization effects and associated properties, so proteins are not contributing factors.

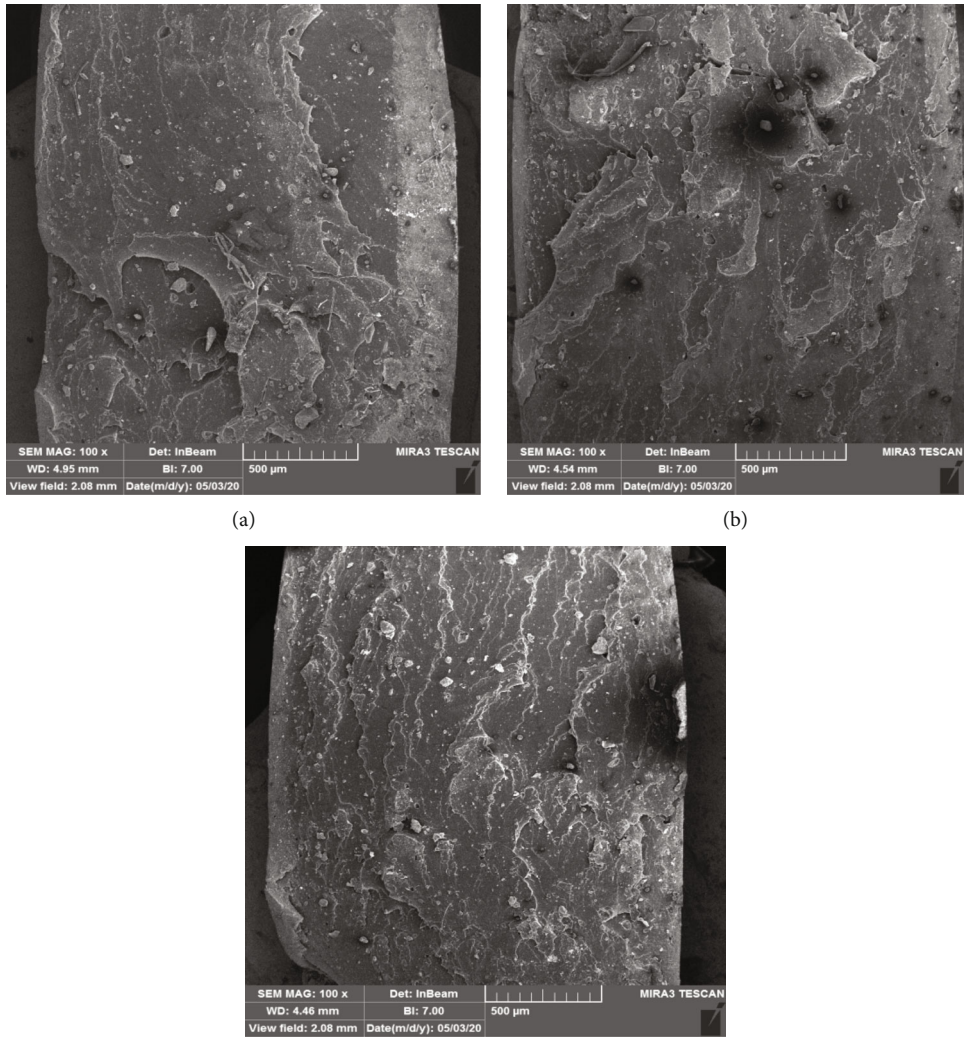

Figure 14: SEM image: (a) 50% strain amplitude for S40N60C5 sample, (b) 60% strain amplitude for S40N60C5 sample, and (c) 70% strain amplitude for S40N60C5 sample.

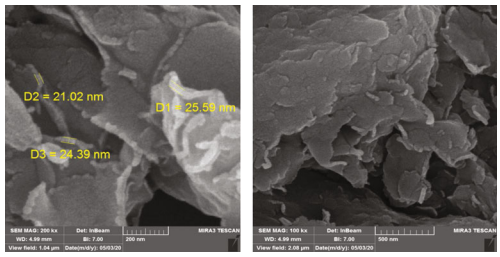

Figure 15: FESEM image of prepared nanoclay powder.

Recently, through a model of cis-polyisoprene joined with stearic acid, it has been shown that sodden fatty acids linked to the rubber chain enforce crystallization, while mixed unsaturated fatty acids, which are existing in NR, act as a plasticizer and accelerate the crystallization rate. Through nuclear magnetic resonance (NMR) studies, the chain ends of NR were detected to contain two trans isoprene units and an oligopeptide at one end and a phospholipid terminative group at the other which matched the crystallinity effects of the stearic acid grafted polyisoprene model above [6]. These polymer terminations may also allow NR to act as a functionalized polymer resulting in branching at the chain ends.

SEM images of S40N60C5 rubber composition fracture surfaces as shown in Figure 14 at 50%, 60%, and 70% strain amplitude, respectively, show that the fracture surface of the specimens becomes smoother as the strain increases. This is due to the presence of cavities and cracks that occur at low strain values at the failure surfaces and cause delays in the failure onset of the specimens and increase their fatigue life, causing rough surfaces in the failure regions of the specimens.

The layered nanoclay consists of quadrilateral and octagonal plates; in quadrilateral plates, a silicon atom is surrounded by four oxygen atoms, and in octagonal plates, eight oxygen atoms enclose a metal atom (such as iron, magnesium, or aluminum). Quadrilateral and octahedral plates combine to form oxygen atoms by sharing oxygen atoms, and noncommon oxygen forms a hydroxyl (OH) agent. There are two types of plate combinations mentioned for nanoclay structure; by replacing

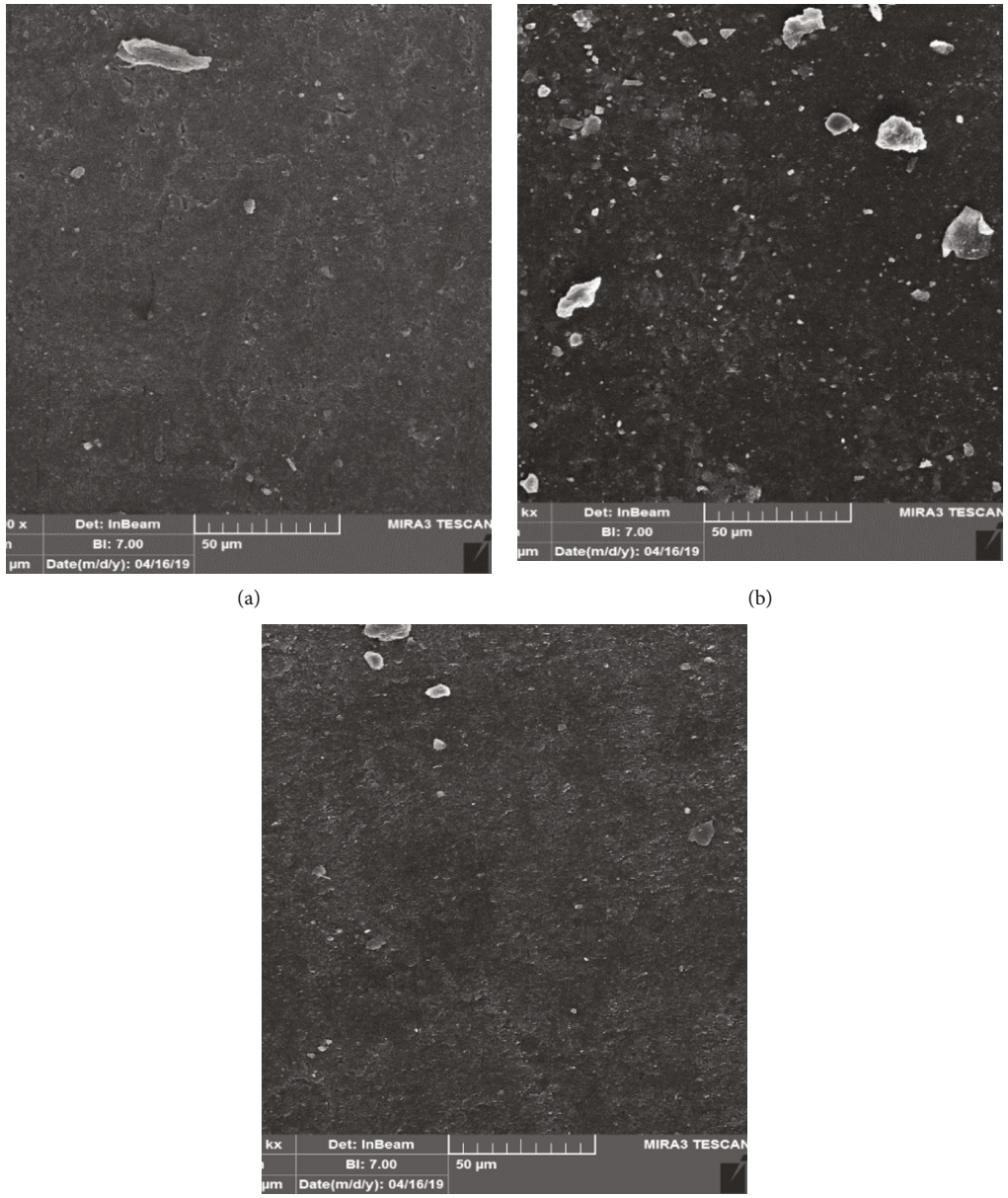

Figure 16: SEM image: (a) S70N30 sample, (b) S70N30C3 sample, and (c) S70N30C5 sample.

different atoms with existing atoms, it is possible to create positive and negative ionic charges between nanoclay layers [37].

Field emission scanning electron microscopy images related to the prepared nanoclay powder are presented in Figure 15.

The forces between the layers are van der Waals and electrostatic forces, which are considered weak forces. Due to the presence of these weak forces as well as the distance between the layers, the cations between the layers can be hydrated in aqueous solutions, causing swelling and increasing the distance between the layers. The thickness of the nanoclay is about 1 nm, and its transverse dimensions can vary from 30 nm to a few microns. The transverse dimensions of the nanoclays and their ability to disperse into individual layers determine the optical coefficient of the nanoclays, which significantly affects the surface reactions. The separation of layers and the creation of nanoclay layers with a thickness of 1 nm are the ideal structures that can dramatically improve the properties of the polymer. On the other hand, in cases where the distribution is well done, the increase of internal surfaces will increase the forces between the monolayers and their tendency to accumulate and clump [37]. The homogeneous dispersion of the nanoclay and the formed filler network can prevent the loss of additional energy during deformation. This helps to resist the dynamic cracking of rubber compounds.

Wu et al. [21] showed that the flexural fatigue life of CB-filled SBR is greatly enhanced by the addition of nanoclay. They

Table 6: Storage modulus of samples.

Temperature (°C)	Storage modulus (MPa)					
	S50N50	S50N50C5	S40N60	S40N60C3	S40N60C5	S40N60C7
-70	1313.15	934.78	633.95	276.55	175.15	230.37
-50	30.68	12.65	45.37	28.38	12.93	10.75
-30	7.39	10.02	8.09	8.21	10.38	8. 62
-10	5.76	8.27	6.75	7.42	9.35	7.48
10	5.39	7.80	6.43	6.72	9.13	6.93
30	5.21	7.56	6.04	6.58	9.02	6.73
50	5.13	7.47	5.37	6.44	8.67	6.57

showed that the addition of nanoclay did not reduce the cross-linking of the rubber compound, but increased the tearing energy. Observation of SEM images of fracture morphology in this study showed that nanoclay particles are superior to CB because they can blunt the crack tip. Figure 16 shows the SEM image of the S70N30, S70N30C3, and S70N30C5 specimens. As can be seen, by adding nanoclay to the combination of NR/SBR, the cohesion in the microstructure of the compound and ultimately the fatigue life is increased.

3.2. Dynamic Mechanical Thermal Analysis of Compositions. To obtain more information about the degree of rubber-nanoclay interaction and consequently the degree of restricted motions of rubber segments and also to obtain more information about the effect of temperature on the mobility of elastomeric segments, DMTA was performed on the prepared compounds.

Table 6 shows the storage modulus values of the studied samples. Storage modulus values above the glass transition temperature of nanocomposites increased acceptably with the increasing amount of nanoclay compared to compositions without reinforcing nanoparticles.

As can be seen from the data presented in Table 6, the storage modulus values for the sample containing 5 phr nanoclay were higher but did not change as it increased. These results are consistent with the higher degree of intercalation/exfoliation and thus the greater contribution of nanoclay in increasing the stiffness of nanocomposite specimens. This indicates that there is good interaction between nanoclay and polymer matrix compared to samples prepared without nanoclay. This may be allocated to the relatively higher surface area and the existence of a higher concentration of surface OH groups.

The increase in loading of nanoclay in the NR/SBR compound leads to a quantized increase in storage modulus compared to NR/SBR compound. The storage modulus of the NR/SBR compound with 5 phr nanoclay showed a drop initially than other samples at the lower temperature region (below −30°C). This may be due to higher nanoclay loading that forms agglomeration at a few spots in the NR/SBR compound. The agglomeration can introduce some voids and pores during the sample preparation [45], which may be responsible for the decrease in the storage modulus value at the lower temperature region. However, the trend changes with increasing temperature (above −30°C) as the compounds containing increasing nanoclay loading in NR/SBR compound showed a quantized increase in storage modulus than that of pure NR/SBR.

Table 7: Glass transition temperature (Tg) of samples.

Row	Chemical material	Tg (°C)
1	S50N50	-34
2	S40N60	-50
3	S50N50C5	-62
4	S40N60C3	-52
5	S40N60C5	-64
6	S40N60C7	-63

The glass transition temperature is the temperature after which the polymer chains begin to move on a larger scale, causing the polymer to change from a hard and glassy state to a softer and more rubbery state, in which the modulus drops several times. The glass transition temperature is negative for rubbers. For this reason, rubbers are soft and flexible at ambient temperatures and are hard and brittle at temperatures below the transition temperature. The glass transition temperatures of the prepared samples are shown in Table 7.

The glass transition temperature of samples containing nanoclay is lower than that of samples that do not contain additives. The lowest glass transfer temperature is related to the S40N60C5 sample. It seems that with increasing nanoparticles in the composition, the glass transition temperature decreased. On the other hand, with increasing the amount of NR, the glass transition temperature of the sample has decreased. Figure 17 shows the dynamic storage modulus as a function of temperature (T) for different samples.

As the temperature decreases, the elastomers become harder and more rigid, and when this temperature reaches the glass transition temperature, they lose their rubber-like properties. Usually, the changes in elastomeric properties are physical and reversible unless they are exposed to a large amount of stress [35].

Figure 18 shows variation in damping coefficient (tanδ) versus temperature for different rubber compositions.

Tanδ was decreased with increasing nanoclay. This can be attributed to the layered structure of the clay (high surface

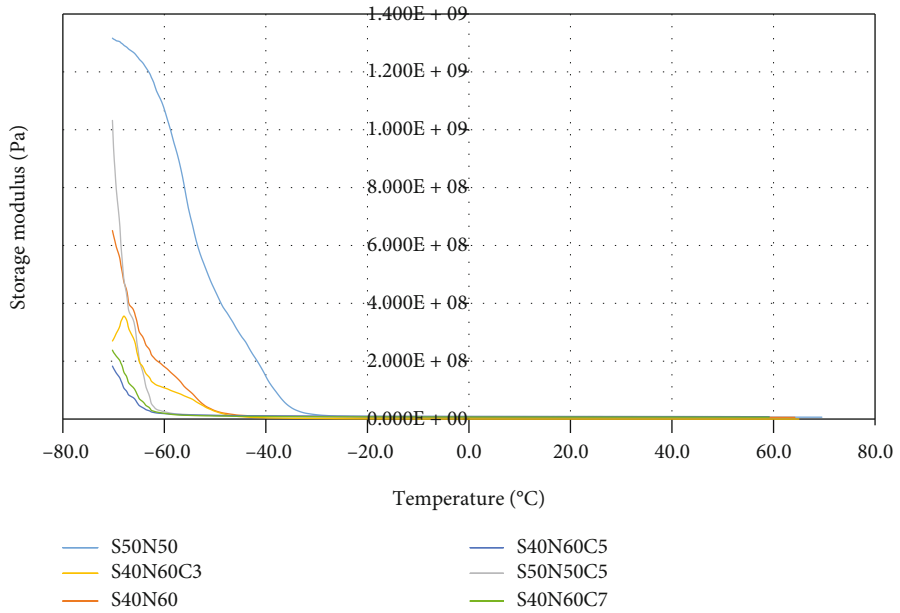

Figure 17: Storage modulus as a function of temperature (T) for rubber samples.

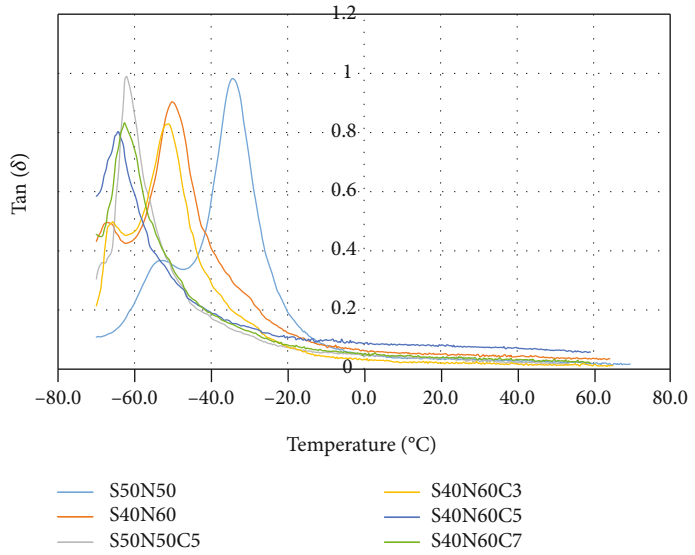

Figure 18: Dynamic loss factor (tanδ) as a function of temperature (T) for rubber samples.

action between the layers) and the stronger adhesion between the nanoclay and the rubber matrix. Decreased tanδ for nanocomposites under low strain amplitude during DMTA analysis also indicates the existence of physical clay networks that resist separation when subjected to short-range strain amplitude. Since the glass transition temperatures of the NR and SBR phases overlap, it is difficult to conclude the difference in the partitioning of the silicate layers between the phases. The lower tanδ for NR/SBR/nanoclay compounds indicates the low strain amplitude resistance of the clay networks, and therefore, the less probability is to changing the direction of the clay nanolayers under the applied dynamic forces [46].

4. Conclusions

In this research, the fatigue life of the NR/SBR compound is evaluated experimentally. The parameters investigated are the NR, SBR, and nanoclay loading in the composition, strain amplitude, and the frequency of the fatigue test. The results of this study showed that by increasing the amount of NR in the rubber composition from 30 to 60 phr, the fatigue life of rubber compositions is more than doubled. For the nanoclay, a threshold value exists beyond which the fatigue life of the rubber compound decreases. The addition of 5 phr nanoclay to S50N50 and S40N60 rubber compositions increases the fatigue life of the

rubber composition by 80% and 117%, respectively. Another important point is that instead of adding nanoclay to the rubber composition, the fatigue life of a compound containing more NR is much longer. NR, due to strain-induced crystallization, increases the size of the crack tip plastic zone and delays the crack growth. As a result, the life of the compound increases. Nanoclay improves the thermodynamic reactions between the rubber polymer chains, which ultimately leads to better nanoclay diffusion within the polymer network. Also, the results of fatigue tests performed at different frequencies show that with increasing the frequency of fatigue tests, the fatigue life of different rubber compositions is reduced due to increased heat generated in the rubber composition. SEM images showed that with increasing strain amplitude value, the failure surface of the samples becomes smoother. The smooth fracture surface indicates that the material failed in the brittle mode. The results of the DMTA analysis, together with the measured mechanical properties, confirmed the results of the fatigue life test.

Data Availability

All data generated or analyzed during this study are included in the manuscript.

Conflicts of Interest

The authors certify that they have no affiliations with or involvement in any organization or entity with any financial or nonfinancial interests in the subject matter or materials discussed in this manuscript.

References

[1] C. Creton and M. Ciccotti, "Fracture and adhesion of soft materials: a review," *Reports on Progress in Physics*, vol. 79, no. 4, article 046601, 2016.

[2] Y. L. Tee, M. S. Loo, and A. Andriyana, "Recent advances on fatigue of rubber after the literature survey by Mars and Fatemi in 2002 and 2004," *International Journal of Fatigue*, vol. 110, pp. 115–129, 2018.

[3] P. Tangudom, S. Thongsang, and N. Sombatsompop, "Cure and mechanical properties and abrasive wear behavior of natural rubber, styrene-butadiene rubber and their blends reinforced with silica hybrid fillers," *Materials & Design*, vol. 53, pp. 856–864, 2014.

[4] J. B. Le Cam and E. Toussaint, "The mechanism of fatigue crack growth in rubbers under severe loading: the effect of stress-induced crystallization," *Macromolecules*, vol. 43, no. 10, pp. 4708–4714, 2010.

[5] B. Huneau, "Strain-induced crystallization of natural rubber: a review of X-ray diffraction investigations," *Rubber Chemistry and Technology*, vol. 84, no. 3, pp. 425–452, 2011.

[6] J. Sakdapipanich and P. Rojruthai, "Molecular structure of natural rubber and its characteristics based on recent evidence," http://cdn.interopen.com/pdfs/29737/InTech-Molecular_structure_of_natural_rubber_and_its_characteristics_based_on_recent_evidence.pdf.

[7] S. M. Cadwell, R. A. Merrill, C. M. Sloman, and F. L. Yost, "Dynamic fatigue life of rubber," *Rubber Chemistry and Technology*, vol. 13, no. 2, pp. 304–315, 1940.

[8] H. Zhang, A. K. Scholz, J. de Crevoisier et al., "Nanocavitation around a crack tip in a soft nanocomposite: a scanning microbeam small angle X-ray scattering study," *Journal of Polymer Science Part B: Polymer Physics*, vol. 53, no. 6, pp. 422–429, 2015.

[9] P. Rublon, B. Huneau, E. Verron et al., "Multiaxial deformation and strain-induced crystallization around a fatigue crack in natural rubber," *Engineering Fracture Mechanics*, vol. 123, pp. 59–69, 2014.

[10] B. Ruellan, J.-B. le Cam, E. Robin et al., "Fatigue crack growth in natural rubber: the role of SIC investigated through post-mortem analysis of fatigue striations," *Engineering Fracture Mechanics*, vol. 201, pp. 353–365, 2018.

[11] L. P. Smith, *The Language of Rubber: An Introduction to the Specification and Testing of Elastomers*, Butterworth-Heinemann Ltd., London, England, 1993, ISBN: 10: 0750614137.

[12] Y. Zhan, N. Yan, G. Fei, H. Xia, and Y. Meng, "Crack growth resistance of natural rubber reinforced with carbon nanotubes," *Journal of Applied Polymer Science*, vol. 137, no. 10, p. 48447, 2020.

[13] Y. P. Wu, Y. Q. Wang, H. F. Zhang et al., "Rubber-pristine clay nanocomposites prepared by co-coagulating rubber latex and clay aqueous suspension," *Science and Technology*, vol. 65, no. 7-8, pp. 1195–1202, 2005.

[14] S. Varghese, K. G. Gatos, A. A. Apostolov, and J. Karger-Kocsis, "Morphology and mechanical properties of layered silicate reinforced natural and polyurethane rubber blends produced by latex compounding," *Journal of Applied Polymer Science*, vol. 92, no. 1, pp. 543–551, 2004.

[15] H. S. Jeon, J. K. Rameshwaram, G. Kim, and D. H. Weinkauf, "Characterization of polyisoprene–clay nanocomposites prepared by solution blending," *Polymer*, vol. 44, no. 19, pp. 5749–5758, 2003.

[16] S. Sadhu and A. K. Bhowmick, "Preparation and properties of styrene–butadiene rubber based nanocomposites: the influence of the structural and processing parameters," *Journal of Applied Polymer Science*, vol. 92, no. 2, pp. 698–709, 2004.

[17] S. K. Lim, J. W. Kim, I.-J. Chin, and H. J. Choi, "Rheological properties of a new rubbery nanocomposite: polyepichlorohydrin/organoclay nanocomposites," *Journal of applied polymer science*, vol. 86, no. 14, pp. 3735–3739, 2002.

[18] Y. P. Wu, Y. Ma, Y. Q. Wang, and L. Q. Zhang, "Effects of characteristics of rubber, mixing and vulcanization on the structure and properties of rubber/clay nanocomposites by melt blending mater," *Macromolecular Materials and Engineering*, vol. 289, pp. 890–894, 2004.

[19] H. Zheng, Y. Zhang, Z. L. Peng, and Y. X. Zhang, "Influence of the clay modification and compatibilizer on the structure and mechanical properties of ethylene–propylene–diene rubber/montmorillonite composites," *Journal of Applied Polymer Science*, vol. 92, no. 1, pp. 638–646, 2004.

[20] M. Arroyo, M. A. Lopez-Manchado, and B. Herrero, "Organo-montmorillonite as substitute of carbon black in natural rubber compounds," *Polymer*, vol. 44, no. 8, pp. 2447–2453, 2003.

[21] W. You-Ping, W. Zhao, and L.-Q. Zhang, "Improvement of flex-fatigue life of carbon-black-filled styrene-butadiene rubber by addition of nanodispersed clay," *Macromolecular Materials and Engineering*, vol. 291, no. 8, pp. 944–949, 2006.

[22] B. Dong, L. Zhang, and Y. Wu, "Influences of different dimensional carbon-based nanofillers on fracture and fatigue

resistance of natural rubber composites," *Polymer Testing*, vol. 63, pp. 281–288, 2017.

[23] Y. Liu, L. Li, Q. Wang, and X. Zhang, "Fracture properties of natural rubber filled with hybrid carbon black/nanoclay," *Journal of Polymer Research*, vol. 18, no. 5, pp. 859–867, 2011.

[24] E. Burgaz, O. Gencoglu, M. Goksuzoglu, and Ondokuz Mayis University, "Carbon black reinforced natural rubber/butadiene rubber and natural rubber/butadiene rubber/styrene-butadiene rubber composites: Part II. Dynamic mechanical properties and fatigue behavior," *Research on Engineering Structures and Materials*, vol. 5, no. 3, 2019.

[25] S. Rooj, A. Das, I. A. Morozov, K. W. Stöckelhuber, R. Stock, and G. Heinrich, "Influence of "expanded clay" on the microstructure and fatigue crack growth behavior of carbon black filled NR composites," *Composites Science and Technology*, vol. 76, pp. 61–68, 2013.

[26] J. A. Gopi, S. K. Patel, A. K. Chandra, and D. K. Tripathy, "SBR-clay-carbon black hybrid nanocomposites for tire tread application," *Journal of Polymer and Research*, vol. 18, no. 6, pp. 1625–1634, 2011.

[27] C. S. Wooa and H. S. Parka, "Fatigue life evaluation of rubber-clay nanocomposites," in *21st European Conference on Fracture, ECF21*, pp. 20–24, Catania, Italy, June 2016.

[28] X. Z. HongyuLi, N. Li, X. Zhang, and A. He, "Influences of crosslinkable crystalline copolymer on the polymer network and filler dispersion of NR/ESBR/CB nanocomposites," *Composites Part A: Applied Science and Manufacturing*, vol. 140, p. 106194, 2021.

[29] S. Cheng, X. Duan, L. Xiaoqing, and Z. Zhang, "Achieving significant thermal conductivity improvement via constructing vertically arranged and covalently bonded silicon carbide nanowires/natural rubber composites," *Journal of Materials Chemistry C*, vol. 9, no. 22, pp. 7127–7141, 2021.

[30] M. Izad, M. T. Ghomi, and G. Pircheraghi, "Increasing the working life and performance improvements of down whole mud motors using nanocomposite elastomer," *Petroleum Research*, vol. 29, pp. 84–94, 2019.

[31] S. Dutta, S. Sengupta, J. Chanda et al., "Distribution of nanoclay in a new TPV/nanoclay composite prepared through dynamic vulcanization," *Polymer Testing*, vol. 83, p. 106374, 2020.

[32] G. Rajeshkumar, S. Arvind Seshadri, and S. Ramakrishnan, "A comprehensive review on natural fiber/nano-clay reinforced hybrid polymeric composites: materials and technologies," *Polymer Composites*, vol. 42, no. 8, pp. 3687–3701, 2021.

[33] K. Zdiri, O. Harzallah, A. Elamri, N. Khenoussi, J. Brendlé, and H. Mohamed, "Rheological and thermal behavior of Tunisian clay reinforced recycled polypropylene composites," *Advances in Polymer Technology*, vol. 37, no. 8, 2018.

[34] K. Prusty, P. K. Sethy, and S. K. Swain, "Sandwich-structured starch-grafted polyethylhexylacrylate/polyvinyl alcohol thin films," *Advances in Polymer Technology*, vol. 37, no. 8, 2018.

[35] M. Morton, *Rubber Technology*, Van Nostrand Reinhold Company, Second edition, 1973.

[36] F. W. Barlow, *Rubber Compounding: Principles, Materials, and Techniques*, Marcell Dekker Inc, 1988.

[37] A. Olad, *Advances in diverse industrial applications of nanocomposites*, BoD–Books on Demand, 2011.

[38] B. Dong, C. Liu, Y. Lu, and Y. Wu, "Synergistic effects of carbon nanotubes and carbon black on the fracture and fatigue resistance of natural rubber composites," *Journal of Applied Polymer Science*, vol. 132, no. 25, p. 25, 2015.

[39] W. Kim, H. Lee, J. Kim, and S.-K. Koh, "Fatigue life estimation of an engine rubber mount," *International Journal of Fatigue*, vol. 26, no. 5, pp. 553–560, 2004.

[40] C.-S. Woo, W.-D. Kim, S. H. Lee, B. I. Choi, and H. S. Park, "Fatigue life prediction of vulcanized natural rubber subjected to heat-aging," *Procedia Engineering*, vol. 1, no. 1, pp. 9–12, 2009.

[41] Q. Li, J. Zhao, and B. Zhao, "Fatigue life prediction of a rubber mount based on test of material properties and finite element analysis," *Engineering Failure Analysis*, vol. 16, no. 7, pp. 2304–2310, 2009.

[42] K. G. Gatos, N. S. Sawanis, A. A. Apostolov, R. Thomann, and J. Karger-Kocsis, "Nanocomposite formation in hydrogenated nitrile rubber (HNBR)/organo-montmorillonite as a function of the intercalant type," *Macromolecular Materials and Engineering*, vol. 289, no. 12, pp. 1079–1086, 2004.

[43] J. A. Kent, "Kent and Riegel's," in *Handbook of Industrial Chemistry and Biotechnology*, p. 16, Springer, Eleventh edition, 2007.

[44] R. Sengupta, S. Chakraborty, S. Bandyopadhyay et al., "A short review on rubber/clay nanocomposites with emphasis on mechanical properties," *Engineering and Science*, vol. 47, no. 11, pp. 1956–1974, 2007.

[45] X. Huang, P. Jiang, C. Kim, Q. Ke, and G. Wang, "Preparation, microstructure and properties of polyethylene aluminum nanocomposite dielectrics," *Composites Science and Technology*, vol. 68, no. 9, pp. 2134–2140, 2008.

[46] M. Andideh, G. Naderi, M. H. R. Ghoreishy, and S. Soltani, "nanocomposites based on NR/SBR: effects of nanoclay and short nylon fibers on the cure characteristics and thermal properties," *Polymer-Plastics Technology and Engineering*, vol. 52, no. 10, pp. 1016–1024, 2013.